Deterministic magnetic moment rotation in antiferromagnetic material by piezoelectric strain modulation

Mengli Liu[1], Chengxin Ma[1], Wei Du[1], Hua Su[1], Huaiwu Zhang[1], Bo Liu[2], Hao Meng[2] and Xiaoli Tang[1]

Abstract

Antiferromagnetic (AFM) spintronic devices play a vital role in the development of novel spintronic devices due to their attractive features. Herein, the interfacial state manipulation of the AFM IrMn material is investigated by combining a ferroelectric single crystal $Pb(Mg_{1/3}Nb_{2/3})_{0.7}Ti_{0.3}O_3$ (PMN-PT) with an electric field (E-field)-controlled magnetic moment arrangement of the IrMn film. A PMN-PT/Cu/IrMn/NiFe heterostructure is chosen to confirm the deterministic manipulation of AFM interfacial states and its angle of magnetic moment rotation. The appropriate thickness of the Cu layer is selected to disrupt the strain-mediated magnetoelectric coupling between the NiFe layer and PMN-PT substrate. The NiFe film reference layer can reflect the variation in AFM interfacial states via the exchange bias. When the E-field is applied, an in-plane piezoelectric strain is produced. If IrMn responds to the strain, its magnetic moment rotates from [001] to [1−10] depending on the crystal orientation of PMN-PT. Based on the experimental results and theoretical analyses, a rotation in the magnetic moment of the IrMn layer by ~20° is confirmed. This work provides convincing evidence for the manipulation of E-field-controlled AFM interfacial states and describes a reliable method for achieving the rotation angle of AFM moments, which can help to accelerate the development of AFM spintronic devices.

Introduction

Antiferromagnetic (AFM) materials with staggered magnetic order and a net magnetic moment of zero are of great interest. They provide promising alternatives to present-day magnetic materials due to their unique features, such as ultrafast spin dynamics, absence of macroscopic magnetization, and insensitivity to external magnetic fields[1,2]. Recently, AFM spintronics was proposed[3], and several studies were conducted to confirm the possibility of the control of AFM moments by the applied electric field (E-field)[4–6]. Several new spin devices and application scenarios[7,8] based on AFM materials have

been proposed to meet the requirements of next-generation information technology.

Numerous investigations are being conducted to devise new methods of controlling the magnetic properties of AFM materials. Several such studies have confirmed that noncollinear antiferromagnets can be modulated by spin current via spin-orbit torque (SOT)[5] and the magneto-electric (ME) effect[9,10], but the number of studies that have utilized controlled collinear AFM alloys is limited. Furthermore, some researchers have questioned the ability of the SOT to switch the AFM Néel vector[11]. The ferroelectric (FE) material-generated piezoelectric strain has received much attention because of its ability to control the magnetism of a ferromagnetic (FM) layer in an FM/FE multiferroic heterostructure[12–14]. Recently, several studies focusing on the piezoelectric strain control AFM magnetic properties have been proposed[9,10,15–19]. The resistance state modulation and Néel SOT manipulation of AFM materials by the E-field were introduced[18,19]. A

Correspondence: Xiaoli Tang (tangtang1227@uestc.edu.cn)
[1]State Key Laboratory of Electronic Thin Films and Integrated Devices, University of Electronic Science and Technology of China, Chengdu, Sichuan 610054, China
[2]Key Laboratory of Spintronics Materials, Devices and Systems of Zhejiang Province, Hangzhou 311305, China

theoretical study of the Néel vector rotation in Mn-based collinear AFM materials has been reported[20]. However, experimental research on controlling their AFM moments by an E-field remains elusive because it is difficult to detect and verify the magnetic states of AFM materials.

In the FM/AFM bilayer, an exchange bias field (H_{eb}) originating from the interfacial exchange coupling effect can be produced[21]. It has been widely applied in spin valves (SVs) and magnetic tunnel junctions (MTJs)[22,23]. The change in H_{eb} also provides an indirect way to display the AFM interfacial state variation[24–27]. Thus, the exchange bias system provides a significant avenue to achieve evidence of AFM interfacial state manipulation by the exchange bias effect. However, in previous studies on AFM modulation using the FM/AFM exchange bias system[27–30], both the FM and AFM materials have large magnetostriction constants. It is difficult to distinguish whether the change in H_{eb} is produced by AFM or FM films or both are responsible for the result. Many $L1_0$-type collinear XMn alloys, such as IrMn and PtMn, have been used in current spintronic devices, and many of them are composed of heavy metals, which can also act as spin electron injection sources via the spin Hall effect[31–33]. Therefore, achieving and verifying their voltage-manipulated AFM moments are critical for AFM-based spintronic devices, and they can be easily made compatible with spintronic devices.

In this work, we determined the E-field controlled AFM moment of IrMn by using a PMN-PT/Cu/IrMn/NiFe exchange-biased heterostructure. When an E-field is applied to the PMN-PT substrate, the piezoelectric strain is transmitted to the AFM IrMn layer but not to the FM NiFe layer due to the strict control of the Cu underlayer thickness. As a result, if the strain causes the AFM magnetic moment to rotate in the [1–10] direction, the magnetic hysteresis (M-H) loops of the bilayer layer can reflect the results. Our experimental results and theoretical calculations confirmed the manipulation of AFM interfacial states by an E-field. An AFM moment rotation of ~20° was obtained. This work develops an important method for obtaining the rotation angles of AFM materials using the exchange bias effect, thus paving the way for the development of AFM spintronic devices.

Materials and methods

To investigate AFM switching, Cu (30–115)/NiFe (12)/Ta (5) and Cu (100)/IrMn (15)/NiFe (12)/Ta (5) (nm) structures were first deposited on a (110)-oriented $Pb(Mg_{1/3}Nb_{2/3})_{0.7}Ti_{0.3}O_3$ (PMN-PT) substrate for comparison. The appropriate thickness of the Cu layer was used to cut off the piezoelectric strain transmission from the PMN-PT substrate to the NiFe film. This experiment provided convincing evidence for the successful modulation of AFM moments by an E-field. The thin films were

deposited by using magnetic sputtering at room temperature with 50 W power and an Ar pressure of 3 mTorr. The easy magnetic axis of the FM layer and the pinning direction were produced initially along the [001] direction by applying a constant magnetic field of 300 Oe during film deposition. $Ni_{80.4}Fe_{19.6}$ was selected as the FM layer due to its small saturation magnetostriction coefficient λ[34,35]. The λ of 2.4×10^{-6} was deduced from the E-field-induced effective magnetic field[36]. During the strain modulation measurements, the E-field was applied along the thickness direction of PMN-PT, and the in-plane magnetization properties of the heterostructures were measured using a vibrating sample magnetometer. All measurements were carried out at room temperature.

Results and discussion

A schematic of the multiferroic heterostructure utilized in the present study is displayed in Fig. 1a. The easy magnetic axis of the FM layer and the pinning direction are initially produced along the [001] direction. The θ, α,
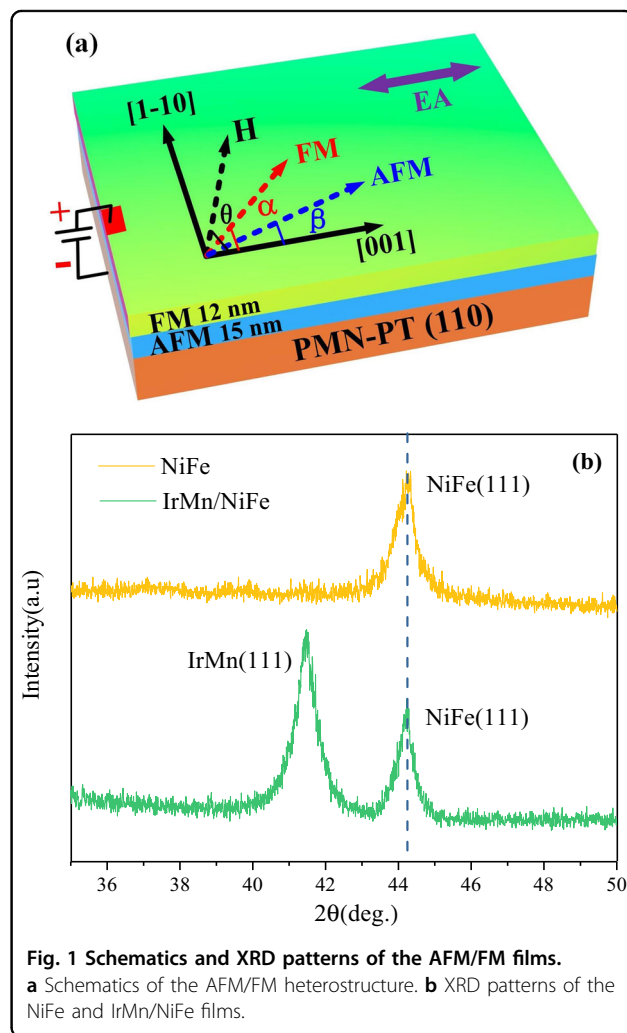

Fig. 1 Schematics and XRD patterns of the AFM/FM films.
a Schematics of the AFM/FM heterostructure. **b** XRD patterns of the NiFe and IrMn/NiFe films.

and β are the measuring angles for the magnetic field, the FM magnetic moment, and the AFM magnetic moment to the [001] direction, respectively. The direction of β is also treated as the direction of the exchange bias field. In a PMN-PT/AFM/FM heterostructure, both the magnetic moment of FM and AFM layers can be controlled by the piezoelectric strain. To study the magnetoelastic effect in the heterostructure, the film quality of the FM and AFM layers was also confirmed. Figure 1b shows the X-ray diffraction (XRD) scans of a single NiFe layer and IrMn/NiFe bilayer. The normal (111) diffraction peaks corresponding to NiFe and IrMn films were obtained[37]. This general polycrystalline texture of the film has been widely used to investigate the ME effect. An effective magnetic field H_{eff} can be produced through the strain-mediated ME coupling between the FM or AFM layer and the PMN-PT substrate, which can be expressed as[36]:

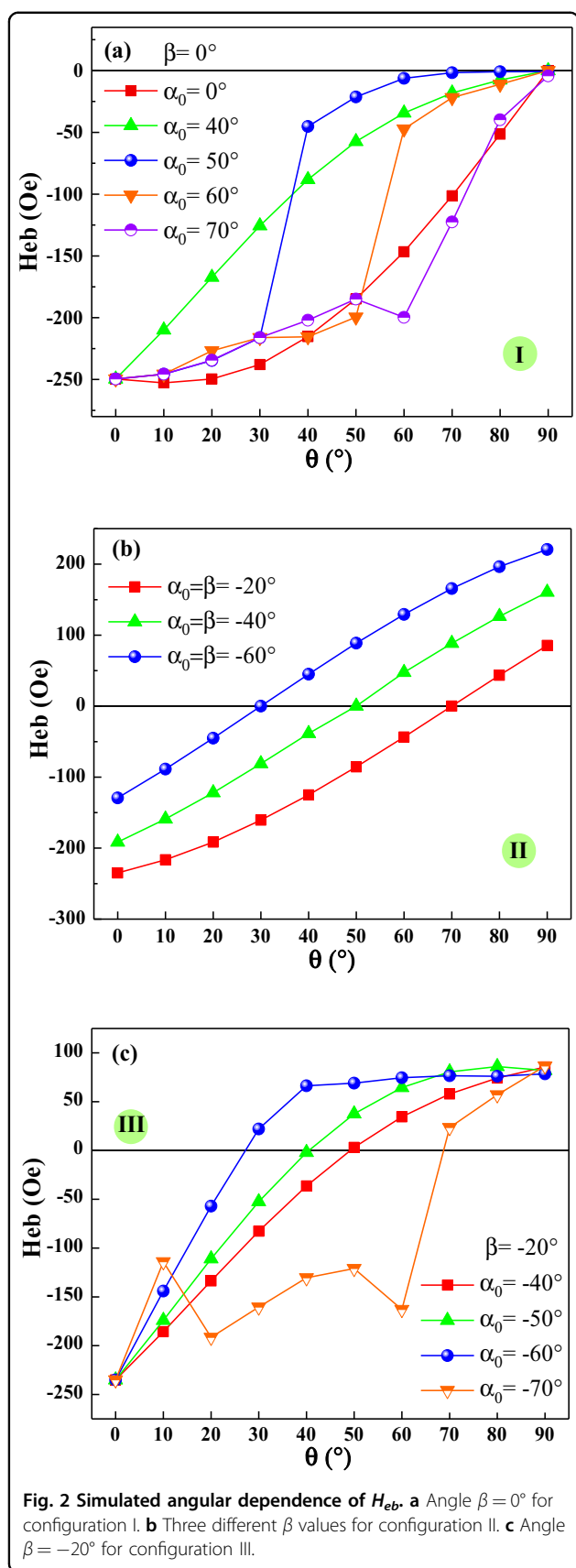$$H_{eff} = \frac{3\lambda(\sigma_{001} - \sigma_{1-10})}{M_S},\qquad(1)$$

where σ_{001} and σ_{1-10} are the in-plane piezo stress values in the [001] and [1–10] directions, λ is the magnetostriction constant, and M_S is the saturated magnetization. Considering a positive magnetostriction constant of NiFe and IrMn[20,34,35] and compressive and tensile strains along the [001] and [1–10] directions, respectively, a positive effective magnetic field along the [1–10] direction is obtained. As a result, the magnetization direction of the FM and AFM layers are rotated toward the [1–10] direction.

To investigate the interfacial state manipulation of the AFM/FM bilayer, we first perform a theoretical analysis by using the Stoner-Wohlfarth model[38]. The free energy density of the exchange-biased system can be expressed as:

$$E = K_U\sin^2(\alpha - \phi) - K_E\cos(\beta - \alpha) - HM\cos(\theta - \alpha),\quad(2)$$

where K_U is the sum of the effective uniaxial anisotropy and the induced uniaxial anisotropy constant of the FM layer, K_E is the unidirectional anisotropy constant originating from the interfacial exchange coupling between FM and AFM layers, and φ is the angle between the effective magnetic field H_{eff} and the [001] direction. Based on the principle of minimal energy, the angle α for the moment, determined by the competition of K_U, K_E and the measuring magnetic field, can be calculated by $\frac{\partial E}{\partial \alpha} = 0$. The corresponding M-H loops were simulated. By changing the direction of the measuring magnetic field, the angular dependence on H_{eb} can be obtained from the simulated M-H loops. Normally, $H_{eb} = 0$ is aligned with the perpendicular direction of the exchange bias field. Therefore, using rotation VSM measurements of H_{eb} in an FM/AFM bilayer and discovering a new direction of
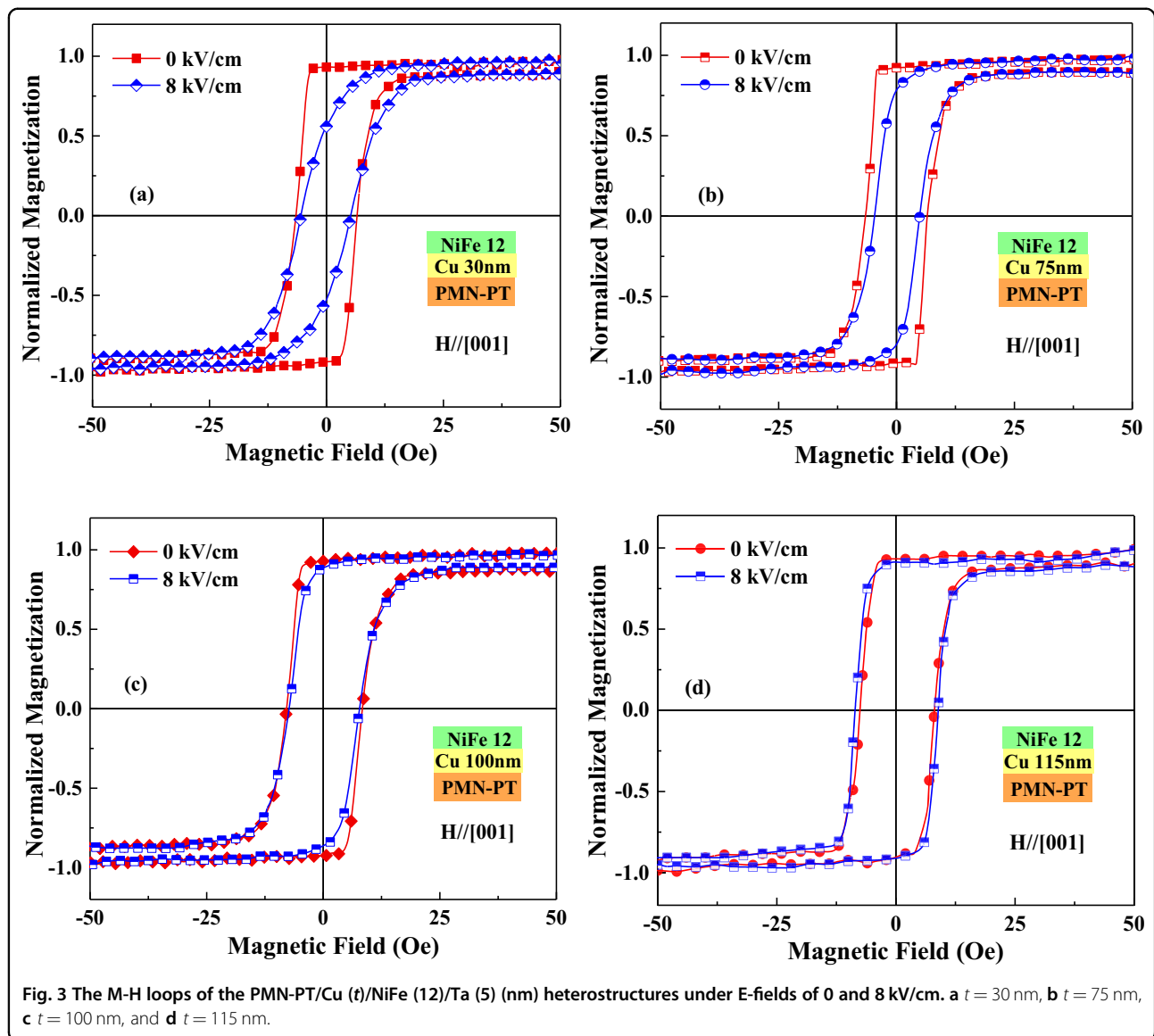
$H_{eb} = 0$ is considered a simple way to achieve a new exchange bias direction and provide effective evidence that the AFM moment was manipulated[24–27]. According to our theoretical calculations, this method has flaws and limitations. The following three configurations are proposed to determine the most effective method. In configuration I, we supposed that only the FM layer would respond to the strain. In configuration II, we assumed that the strain modulates the AFM, and the FM layer does not respond to the strain and instead follows the rotation of the AFM material by the exchanging coupling effect[39]. In configuration III, we considered that both FM and AFM respond to the strain, but their rotation angles are different because of their different magnetostriction constants. The simulated M-H loops in three configurations are shown in Figs. S1, S2, and S3. The $K_E = H_{eb}M_S$[40] is equal to 28,000 J/m³ assuming $H_{eb} = 19778$ A/m and using $M_S = 1.1 \times 10^6$ A/m for the FM film. The initial deviated FM angle is defined as α_0, and it deviates from the [001] direction at an external field of zero. It is determined by the competition between K_U and K_E. We obtained various assumed angles α_0 by calculating particular values of K_U in the simulation. The simulated H_{eb} at the different orientations of the external magnetic fields is displayed in Fig. 2a–c. H_{eb} was found to have a strong angle θ dependence (corresponding to the direction of the measuring field). In the simulations, we defined $\beta = 0°$ for configuration I, three different β values were assumed for modulation of strain in configuration II, and $\beta = -20°$ for configuration III. As shown in Fig. 2a, the determined H_{eb} values at $\alpha_0 = 40°$, 50°, 60°, and 70° were different from those obtained in the initial state ($\alpha_0 = 0°$). In particular, $H_{eb} = 0$ was obtained within a relatively wide region at $\alpha_0 = 50°$. The AFM moments were not modulated in this case. Therefore, relying solely on the angle variation of H_{eb} to confirm the strain or spin current modulation of AFM interfacial states and the direction of $H_{eb} = 0$ to determine the new exchange bias field direction is difficult and inaccurate. Furthermore, similar results were obtained for configuration III. In this case, the AFM moments were assumed to be manipulated by the strain and were aligned at $-20°$. Because the FM and AFM layers respond differently to strain, the FM layer was rotated at a different angle. As shown in Fig. 2c, $H_{eb} = 0$ was obtained at different angles, which contradicts the assumption that the AFM moment was aligned to $-20°$. Therefore, unlike previous reports[27], we cannot simply use the change in exchange-biased curves and the direction perpendicular to $H_{eb} = 0$ to judge the modulation of the AFM interfacial state. In these complex situations, it is difficult to use M-H loops to accurately determine the new direction of the AFM moment when we are not sure whether the AFM moments are modulated or not. In contrast, as displayed

Fig. 2 Simulated angular dependence of H_{eb}. a Angle $\beta = 0°$ for configuration I. **b** Three different β values for configuration II. **c** Angle $\beta = -20°$ for configuration III.

in Fig. 2b, we assumed that the FM layer did not respond to the strain and rotated coherently with the AFM. As shown in Fig. 2b, $H_{eb} = 0$ exactly achieved the direction perpendicular to the AFM magnetic moment. Under this condition, the rotation measurements of the M-H curves can be used to confirm the modulation of interfacial AFM states and determine its new magnetic moment direction from $H_{eb} = 0$. Therefore, we chose the appropriate thickness of the Cu underlayer to cut off the transmission of piezoelectric strain to the FM film while matching configuration II. If the modulated M-H loops are achieved, it provides conclusive evidence of strain control of AFM interfacial states and the rotation angle of the AFM moments.

The magnetization direction of the FM layer does not respond to the piezoelectric strain to match model configuration II. We inserted a thick Cu layer between the NiFe film and PMN-PT substrate to cut off their strain-mediated ME coupling effect. Figure 3 displays the M-H loops of the PMN-PT/Cu (t)/NiFe (12)/Ta (5) (nm) multiferroic heterostructures with and without an E-field for different thicknesses of the inserted Cu layer. The thickness of the Cu layer was in the range of 30–115 nm. The measuring magnetic field was applied in the [001] direction, which corresponds to the easy axis of the NiFe film. Although the magnetostriction constant of NiFe is very small, it still responds to the large strain produced by PMN-PT when the thickness of Cu is 30 nm (Fig. 3a). This result indicates that the easy axis of the NiFe film is rotated toward the [1–10] direction due to ME coupling. The response to the strain decreases as the thickness of the Cu layer is increased. When the thickness of Cu reaches 115 nm, there is little difference between the M-H loops measured at the E-field of 0 kV/cm and 8 kV/cm (Fig. 3d), indicating that the impact of the piezoelectric strain on the FM layer has been eliminated.
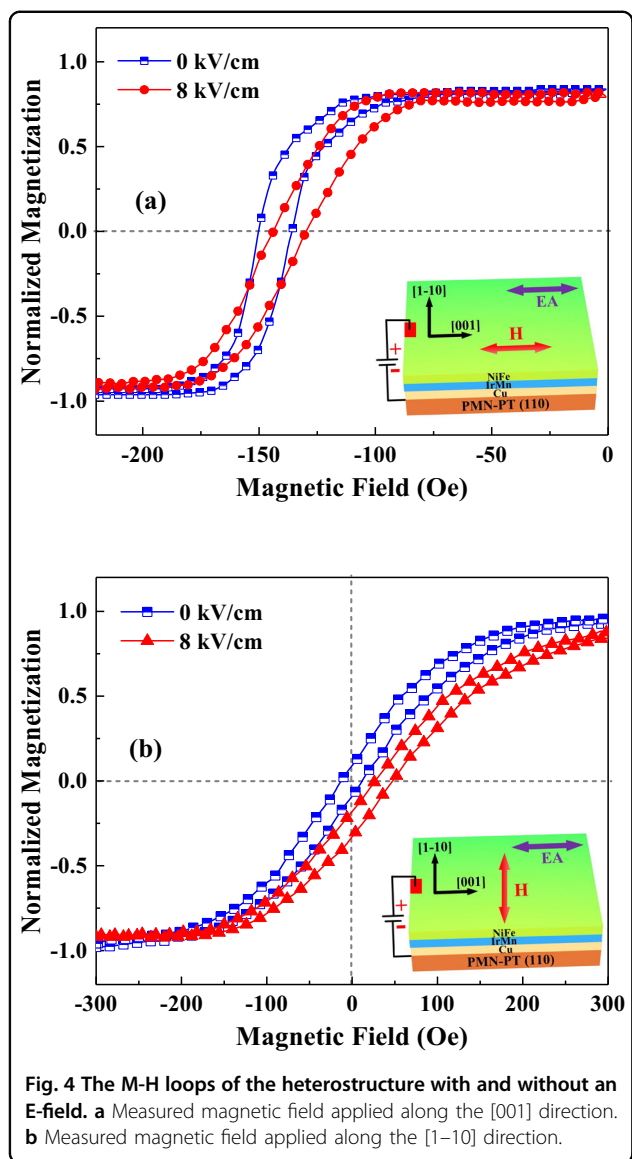
According to the above experiments, a 115 nm inserted Cu layer is enough to isolate the impact of strain on the FM layer. Therefore, a PMN-PT/Cu (100)/IrMn (15)/NiFe (12)/Ta (5) (nm) multiferroic heterostructure was fabricated to investigate the modulation of AFM IrMn film by the ME effect. Figure 4 presents the E-field dependence of the M-H loops of the magnetic field measured in the [001] and [1–10] directions. In the initial state, because the pinning direction was along the [001] direction, a straight loop with large H_{eb} and a slanted loop without H_{eb} were obtained when the measuring magnetic field was parallel and perpendicular to the AFM magnetic moment. The M-H loops changed when an E-field of 8 kV/cm was applied. As shown in Fig. 4a, when the external magnetic field was applied in the direction of the initial exchange bias, the H_{eb} decreased by ~10%, and the M-H curve showed a slanted loop. In contrast, a slanted M-H loop with a positive H_{eb} was obtained in the initial $H_{eb} = 0$

Fig. 3 The M-H loops of the PMN-PT/Cu (*t*)/NiFe (12)/Ta (5) (nm) heterostructures under E-fields of 0 and 8 kV/cm. a *t* = 30 nm, **b** *t* = 75 nm, **c** *t* = 100 nm, and **d** *t* = 115 nm.

direction ([1−10] direction), as shown in Fig. 4b. Because the E-field does not affect the magnetic properties of the NiFe layer due to the inserted Cu layer, such a variation in H_{eb} was attributed to the changing interfacial states of the IrMn layer. The repeated measurements of M-H loops in the other two heterostructure samples are displayed in Figs. S4 and S5. The measurements taken when the voltage in the sample was turned on and off multiple times are displayed in Fig. S6. These measurements confirmed that the E-field-controlled AFM interfacial state manipulation is repeatable and reliable. These results indicate that the magnetic moment of the IrMn layer was changed from the [001] to [1−10] direction by the piezoelectric strain. The AFM rotational direction was consistent with the result predicted by Eq. (1) because the λ of IrMn is positive[20] and $\sigma_{001} - \sigma_{1-10}$ is negative. Then, a H_{eff} that
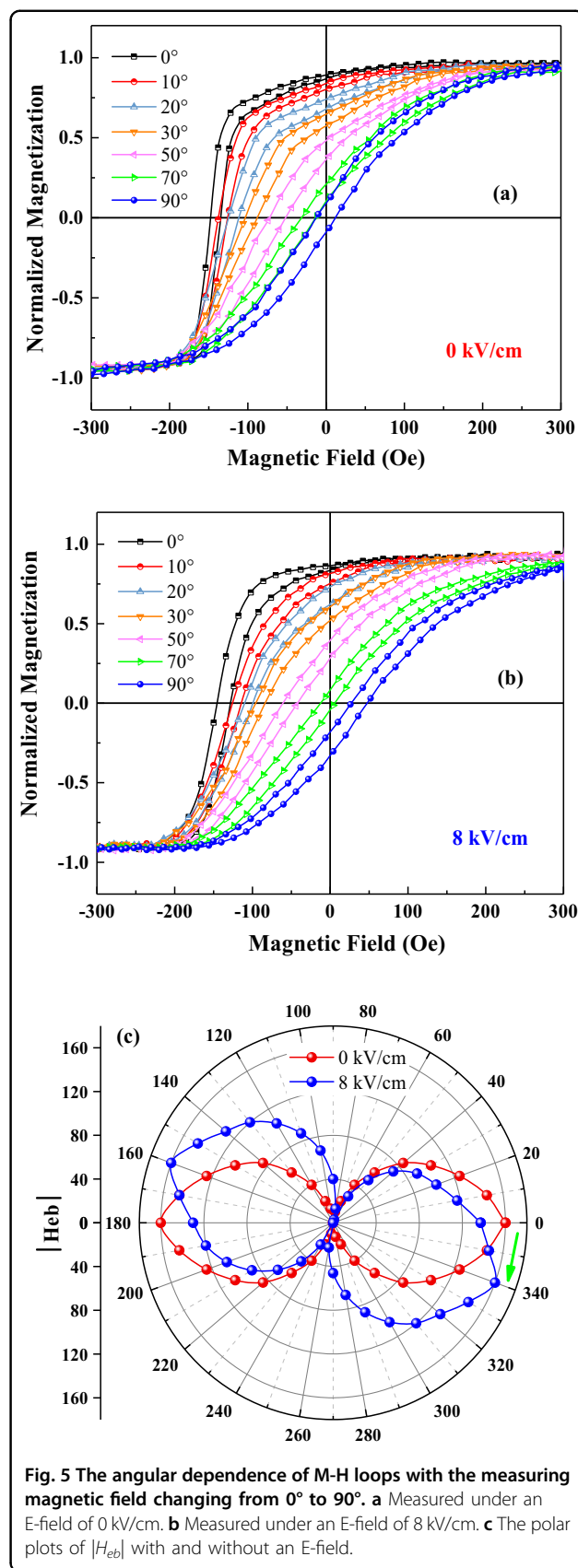
represents an effective field along the [1−10] direction was introduced; such a field can rotate the magnetic moment of the AFM layer in the [1−10] direction due to the strain-mediated ME effect.
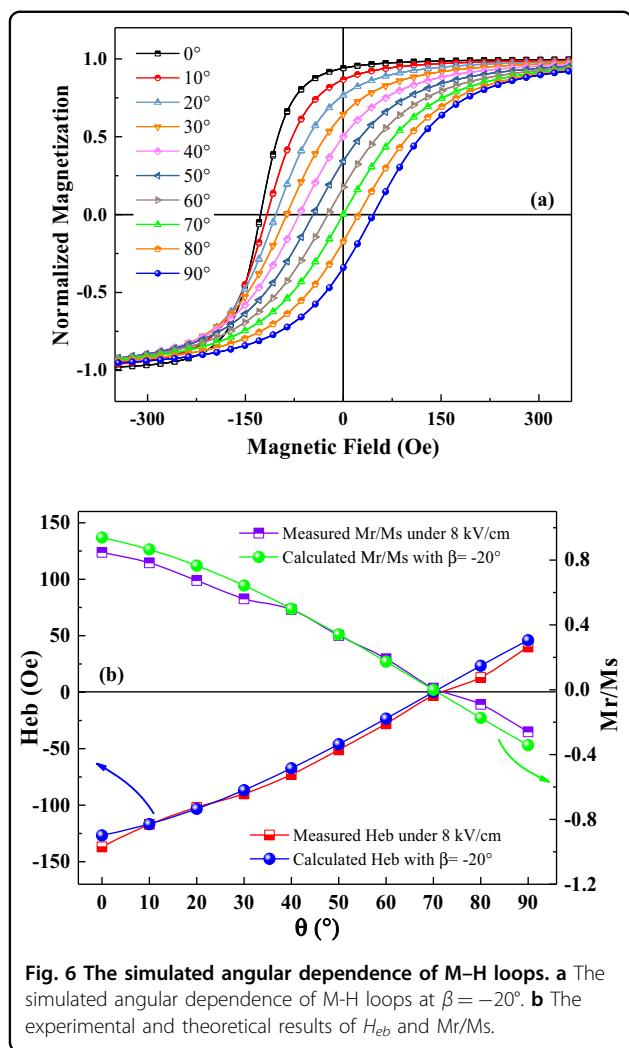
Based on the results displayed in Fig. 4, the deterministic AFM moment rotation in IrMn by piezoelectric strain was confirmed. To gain deeper insight into the modulating results, the angular dependence of M-H loops with and without an E-field was also measured to gain a better understanding of the modulating process. As shown in Fig. 5a, the angular dependence of the M-H loops without an E-field is displayed for the measuring magnetic fields applied along different directions (0° to 90°). H_{eb} decreased with increasing angle θ from 0° to 90°, and this trend is consistent with normal exchange-biased theory and experiments[24,25]. $H_{eb} = 0$ at 90° when

Fig. 4 The M-H loops of the heterostructure with and without an E-field. a Measured magnetic field applied along the [001] direction. **b** Measured magnetic field applied along the [1−10] direction.

Fig. 5 The angular dependence of M-H loops with the measuring magnetic field changing from 0° to 90°. a Measured under an E-field of 0 kV/cm. **b** Measured under an E-field of 8 kV/cm. **c** The polar plots of |H_{eb}| with and without an E-field.

the applied magnetic field was perpendicular to the exchange bias direction. The angular dependence of the M-H loops measured under an E-field of 8 kV/cm was displayed in Fig. 5b. H_{eb} decreased to zero at $\theta = 70°$, and a nonzero H_{eb} was obtained at $\theta = 90°$. The angular dependence of H_{eb} in the FM/AFM bilayer indicated that the magnetic moment of the IrMn film was rotated by −20° from [001] to [1−10] by the E-field. The polar plots of H_{eb} versus θ are also displayed in Fig. 5c. The initial exchange bias direction is aligned along 0°, and the green single arrow represents the rotation direction of AFM moments. When an E-field of 8 kV/cm was applied, the magnetic moment of the IrMn film was rotated to the −20° (340°) direction.

Theoretical calculations using Eq. (2) were performed to further confirm the magnetic moment rotation of the

Fig. 6 The simulated angular dependence of M–H loops. a The simulated angular dependence of M-H loops at $\beta = -20°$. **b** The experimental and theoretical results of H_{eb} and Mr/Ms.

multiferroic heterostructure. The Cu underlayer was used to disrupt the strain-mediated ME coupling between the NiFe layer and the PMN-PT substrate. In this case, the variation in the M-H loops of the pinned NiFe layer indicated the manipulation of interfacial states of the IrMn layer. By applying an E-field, the piezoelectric strain produced rotation of the IrMn moment toward the [1–10] direction was confirmed. The experimental results and theoretical calculations indicated that the magnetic moment rotation of the IrMn layer was 20°. These results demonstrate deterministic AFM moment manipulation controlled by the piezoelectric strain and a method to determine the modulated angle of the AFM moments. This research suggests that the piezoelectric strain can be used to control the magnetic properties of AFM materials and has great potential for developing low-power AFM spintronic devices.

Author contributions
M.L.L. and X.L.T. conceived and designed the experiments. M.L.L., C.X.M., and W.D. performed theoretical calculations. C.X.M., B.L., and H.M. obtained experimental data. M.L.L., H.S., H.W.Z., and X.L.T. analyzed the experimental and theoretical results. M.L.L. and X.L.T. wrote the manuscript after discussion with all the authors. X.L.T. supervised the entire project.

Data availability
All data that support the findings of this study are included within the article.

Conflict of interest
The authors declare no competing interests.

IrMn film. Figure 6a displays the simulated M-H loops when the measuring magnetic field was varied from 0° to 90°. The strain was assumed to modulate the angle β to −20°, and the magnetic moment of the FM layer is coherently rotated with AFM. The simulated results are consistent with the measured results shown in Fig. 5b. In addition, the consistent experimental data with the simulated results were also repeated successfully on several other similar heterostructure samples. They confirmed the correctness of the research. The experimental and simulated results for different directions of the applied fields are plotted in Fig. 6b. The simulated data and the measured results were in good agreement. The zero H_{eb} and the minimum Mr/Ms were obtained at $\theta = 70°$, which demonstrates that the AFM magnetic moment was rotated ~20° by a piezoelectric strain.

Conclusions
In summary, we investigated the interfacial state manipulation of AFM IrMn in a PMN-PT/Cu/IrMn/NiFe

References
1. Jungwirth, T., Marti, X., Wadley, P. & Wunderlich, J. Antiferromagnetic spintronics. *Nat. Nanotechnol.* **11**, 231–241 (2016).
2. Baltz, V. et al. Antiferromagnetic spintronics. *Rev. Mod. Phys.* **90**, 015005 (2018).
3. Gomonay, O., Jungwirth, T. & Sinova, J. Concepts of antiferromagnetic spintronics. *Phys. Status Solidi RRL* **11**, 1700022 (2017).
4. Wadley, P. et al. Electrical switching of an antiferromagnet. *Science* **351**, 587–590 (2016).
5. Hajiri, T., Ishino, S., Matsuura, K. & Asano, H. Electrical current switching of the noncollinear antiferromagnet Mn₃GaN. *Appl. Phys. Lett.* **115**, 052403 (2019).
6. Bodnar, S. Y. et al. Writing and reading antiferromagnetic Mn₂Au by Néel spin-orbit torques and large anisotropic magnetoresistance. *Nat. Commun.* **9**, 348 (2018).
7. Park, B. G. et al. A spin-valve-like magnetoresistance of an antiferromagnet-based tunnel junction. *Nat. Mater.* **10**, 347–351 (2011).

8. Kosub, T. et al. Purely antiferromagnetic magnetoelectric random access memory. *Nat. Commun.* **8**, 13985 (2017).

9. Liu, Z. Q. et al. Electrical switching of the topological anomalous Hall effect in a noncollinear antiferromagnet above room temperature. *Nat. Electron.* **1**, 172–177 (2018).

10. Wang, X. N. et al. Integration of the noncollinear antiferromagnetic metal Mn_3Sn onto ferroelectric oxides for electric-field control. *Acta Materialia* **181**, 537–543 (2019).

11. Chiang, C. C., Huang, S. Y., Qu, D., Wu, P. H. & Chien, C. L. Absence of evidence of electrical switching of antiferromagnetic Néel vector. *Phys. Rev. Lett.* **123**, 227203 (2019).

12. Chen, A. T. & Zhao, Y. G. Progress of converse magnetoelectric coupling effect in multiferroic heterostructures. *Acta Phys. Sin.* **67**, 157513 (2018).

13. Hu, J. M., Chen, L. Q. & Nan, C. W. Multiferroic heterostructures integrating ferroelectric and magnetic materials. *Adv. Mater.* **28**, 15–39 (2016).

14. Song, C., Cui, B., Li, F., Zhou, X. J. & Pan, F. Recent progress in voltage control magnetism: materials, mechanisms, and performance. *Prog. Mater. Sci.* **87**, 33–82 (2017).

15. Feng, Z., Yan, H. & Liu, Z. Electric-field control of magnetic order: from FeRh to topological antiferromagnetic spintronics. *Adv. Electron. Mater.* **5**, 1800466 (2019).

16. Liu, Z. Q. et al. Antiferromagnetic piezospintronics. *Adv. Electron. Mater.* **5**, 1900176 (2019).

17. Zhao, T. et al. Electrical control of antiferromagnetic domains in multiferroic $BiFeO_3$ films at room temperature. *Nat. Mater.* **5**, 823–829 (2006).

18. Yan, H. et al. A piezoelectric, strain-controlled antiferromagnetic memory insensitive to magnetic fields. *Nat. Nanotechnol.* **14**, 131–136 (2019).

19. Chen, X. Z. et al. Electric field control of Néel spin-orbit torque in an antiferromagnet. *Nat. Mater.* **18**, 931–935 (2019).

20. Park, I. J. et al. Strain control of the Néel vector in Mn-based antiferromagnets. *Appl. Phys. Lett.* **114**, 142403 (2019).

21. Nogues, J. & Schuller, I. K. Exchange bias. *J. Magn. Magn. Mater.* **192**, 203–232 (1999).

22. Binasch, G., Grünberg, P., Saurenbach, F. & Zinn, W. Enhanced magnetoresistance in layered magnetic structures with antiferromagnetic interlayer exchange. *Phys. Rev. B* **39**, 4828(R) (1989).

23. Parkin, S. S. P. et al. Exchange-biased magnetic tunnel junctions and application to nonvolatile magnetic random access memory. *J. Appl. Phys.* **85**, 5828–5833 (1999).

24. Ambrose, T., Sommer, R. L. & Chien, C. L. Angular dependence of exchange coupling in ferromagnet/antiferromagnet bilayers. *Phys. Rev. B* **56**, 83–86 (1997).

25. Da Silva, R. B. et al. Angular dependence of asymmetric magnetoimpedance in exchange biased NiFe/IrMn multilayers. *Appl. Phys. Lett.* **104**, 102405 (2014).

26. Tang, X. L., Zhang, H. W., Su, H., Zhong, Z. Y. & Jing, Y. L. Changing and reversing the exchange bias in a current-in-plane spin valve by means of an electric current. *Appl. Phys. Lett.* **91**, 122504 (2007).

27. Sheng, P. et al. Magnetoelastic anisotropy of antiferromagnetic materials. *Appl. Phys. Lett.* **115**, 242403 (2019).

28. Zhang, Y. J. et al. Ferroelectric strain modulation of antiferromagnetic moments in Ni/NiO ferromagnet/antiferromagnet heterostructures. *Phys. Rev. B* **95**, 174420 (2017).

29. Zhang, E. Z. et al. Manipulating antiferromagnetic interfacial states by spin-orbit torques. *Phys. Rev. B* **104**, 134408 (2021).

30. Lin, P. H. et al. Manipulating exchange bias by spin-orbit torque. *Nat. Mater.* **18**, 335–341 (2019).

31. Hou, D., Qiu, Z & Saitoh, E. Spin transport in antiferromagnetic insulators: progress and challenges. *NPG Asia Mater.* **11**, 35 (2019).

32. Frangou, L. et al. Enhanced spin pumping efficiency in antiferromagnetic IrMn thin films around the magnetic phase transition. *Phys. Rev. Lett.* **116**, 077203 (2016).

33. Wang, X. et al. Spin transmission in IrMn through measurements of spin Hall magnetoresistance and spin-orbit torque. *Phys. Rev. B* **101**, 144412 (2020).

34. Klokholm, E. & Aboaf, J. A. The saturation magnetostriction of permalloy films. *J. Appl. Phys.* **52**, 2474 (1981).

35. Kim, Y. K. & Silva, T. J. Magnetostriction characteristics of ultrathin permalloy films. *Appl. Phys. Lett.* **68**, 2885 (1996).

36. Liu, M. et al. Electrical tuning of magnetism in Fe_3O_4/PZN-PT multiferroic heterostructures derived by reactive magnetron sputtering. *J. Appl. Phys.* **107**, 073916 (2010).

37. Devasahayam, A. J., Sides, P. J. & Kryder, M. H. Magnetic, temperature, and corrosion properties of the NiFe/IrMn exchange couple. *J. Appl. Phys.* **83**, 7216 (1998).

38. Stoner, E. C. & Wohlfarth, E. P. A mechanism of magnetic hysteresis in heterogeneous alloys. *Philos. Trans. R. Soc. Lond., Ser. A* **240**, 826 (1948).

39. Grady, K. O. ', Fernandez-Outon, L. E. & Vallejo-Fernandez, G. A new paradigm for exchange bias in polycrystalline thin films. *J. Magn. Magn. Mater.* **322**, 883 (2010).

40. Camarero, J. et al. Origin of the asymmetric magnetization reversal behavior in exchange-biased systems: competing anisotropies. *Phys. Rev. Lett.* **95**, 057204 (2005).